2

Fabrication of paper-based substrate for detection and analysis of pharmaceuticals drugs in water

Present chapter describes the fabrication of a low-cost SERS substrate using printing grade paper as a platform. Characterization techniques like FESEM and TEM have been used to study the surface morphology of the fabricated SERS platform and the synthesized nanoparticles. SERS signature of two standard Raman probes MG and R6G has been investigated. Further this following this SERS analysis of two commonly used pharmaceuticals drugs paracetamol and aspirin have been investigated in real water samples.

2.1 Introduction

The quest for designing affordable and sensitive SERS platform has becoming an attractive field of research in the recent years. The real challenge lies in the development of a reliable SERS platform using a simple yet low-cost modality to be used as a viable alternative to the commercial counterparts. Several low-cost substrate fabrication routes like Blu-ray DVD [1], filter paper [2], leaf [3, 4], nanofiber [5] based substrates have been explored with the focus of application in various chemical and biosensing areas. The printing grade paper serves as a good alternative platform which could be used as a low-cost SERS platform. The printing grade papers are identified by the grams per square meter (GSM) which designates the grams of raw materials (here cellulose) which was used for the fabrication of the paper. The characteristics of paper, such as its grade, thickness, porosity, and roughness, can affect its surface morphology at a submicro level which means that achieving a uniform surface on paper is a challenging task. As a result, the diffusion of metal nanoparticles in colloidal form can vary depending on the GSM-grade paper substrate being used. Due to the appropriate proportion of the in-plane diffusion over the lateral

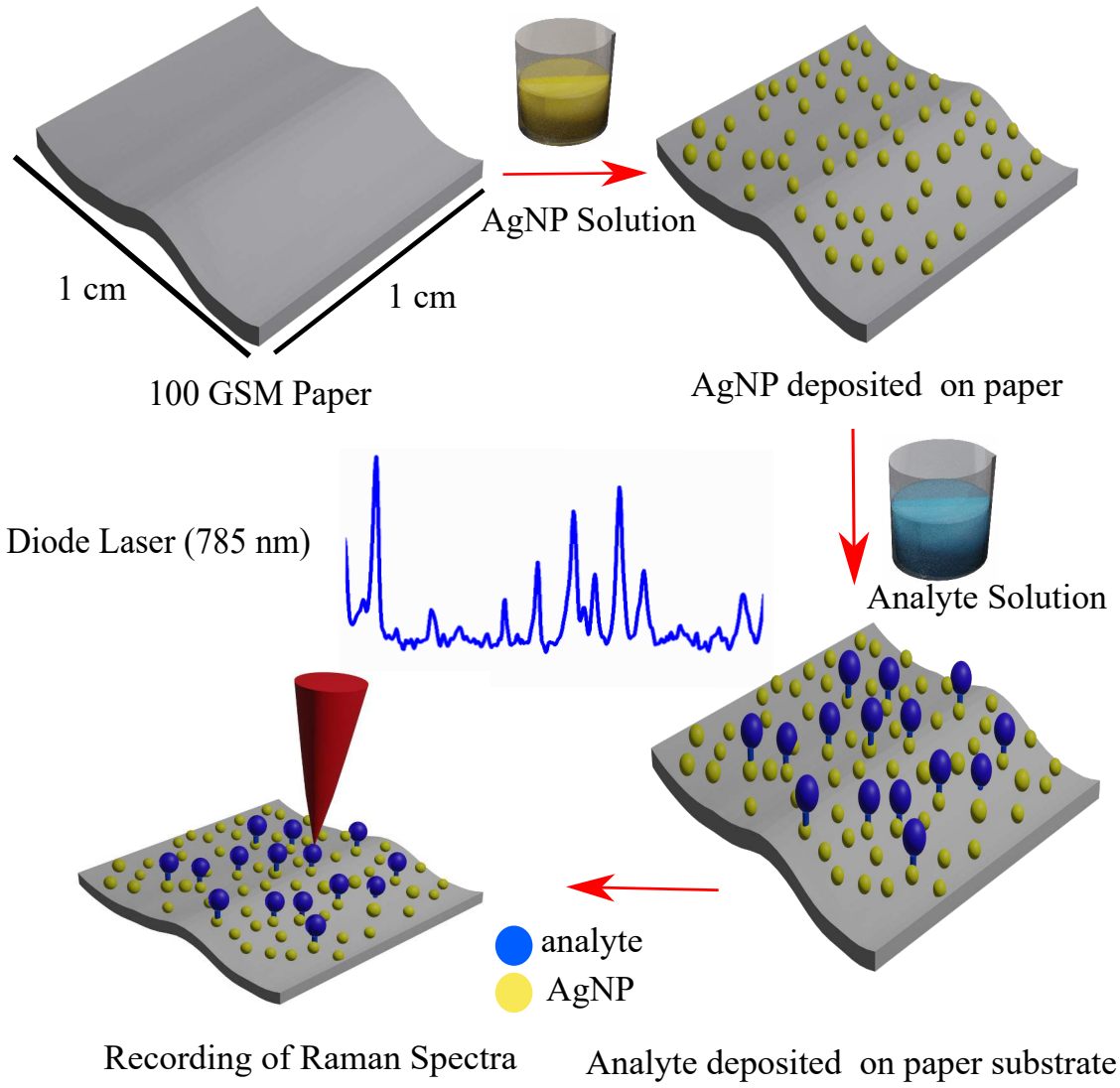

Figure 2.1: Schematic of the experimental setup

diffusion, 100 GSM papers substrates are observed to provide enhanced SERS characteristics [6]. In this study, 100 GSM was utilized as a base for development of a SERS substrate. The usability of the proposed SERS platform has been used for rapid and accurate detection of pharmaceutical drugs in an aqueous environment. The schematic representation of the experimental work is depicted in figure 2.1. The proposed substrate was fabricated by drop-casting a solution of colloidal AgNPs onto 100 GSM paper. After drying at room temperature for approximately 6 hours, this substrate was employed for detecting R6G and MG test samples.

The presence of pharmaceutical in natural water resources posses serious health threat to humans as well as aquatic animals. The widely used over the counter drugs falling into this category are paracetamol and aspirin. So, in the final step of this re-

search work the fabricated low-cost paper substrate has been employed to detect these pharmaceuticals in real water samples. Paracetamol, also known as acetaminophen and 4-hydroxyacetanilide, is a widely used analgesic and antipyretic drug. Like other pharmaceuticals in its class, it is rapidly absorbed and distributed after oral intake and is readily excreted in urine [7, 8]. Studies have shown that these pharmaceutical components are not completely eliminated during wastewater treatment nor entirely biodegraded [9–12]. Conventional water treatment methods such as chlorination can result in the formation of toxic intermediates [13, 14]. Aspirin, another significant medication, is a widely used nonsteroidal anti-inflammatory drug known for its antipyretic and analgesic properties [15–17]. It has been identified as a source of micropollutants in river water and other bodies of water due to various sources of disposal [18]. Studies have shown that aspirin remains unaffected by chlorination [19]. While low doses of aspirin can prevent cardiovascular disease, prolonged use may lead to gastrointestinal issues [20]. Chronic ingestion can also result in salicylate poisoning due to the accumulation of salicylic acid in the bloodstream [21]. Several groups have reported SERS-based detection of paracetamol using different substrates such as colloidal AuNPs drop-cast onto microscopic glass slides [22], dispensed AuNPs on aluminum foil [23], molecularly imprinted polymers [24], or transparent nanostructured surfaces produced lithography-free [25]. Similarly, aspirin detection has been performed on spiked urine samples using an in situ laser-induced photochemical silver substrate synthesized in a moving flow cell [26], in blood serum utilizing colloidal NP solutions of silver and gold [27], on silver nets sputtered on porous silicon [28], and with NP-coated filter paper [29]. The limit of detection (LoD) for both analytes was observed to be 0.1 mM, surpassing some earlier reported results [22–27].

2.2 Experimental

2.2.1 Materials

Silver nitrate ($AgNO_3$) and trisodium citrate ($C_6H_5Na_3O_7$) were obtained from Merck, India. MG and R6G were purchased from Alpha Aesar, India. Paracetamol ($C_8H_9NO_2$) and aspirin ($C_9H_8O_4$) were procured from Acros Organics. All chemicals were utilized without any additional processing

2.2.2 Synthesis of colloidal AgNP

Employing the established Lee-Meisel method detailed elsewhere [27], colloidal AgNP solution was synthesized in the laboratory. In this approach, trisodium citrate functions both as a reducing agent and a stabilizer. Initially, 100 mL of 1 mM $AgNO_3$ solution was brought to boiling temperature. Subsequently, 4 mL of a 1% trisodium

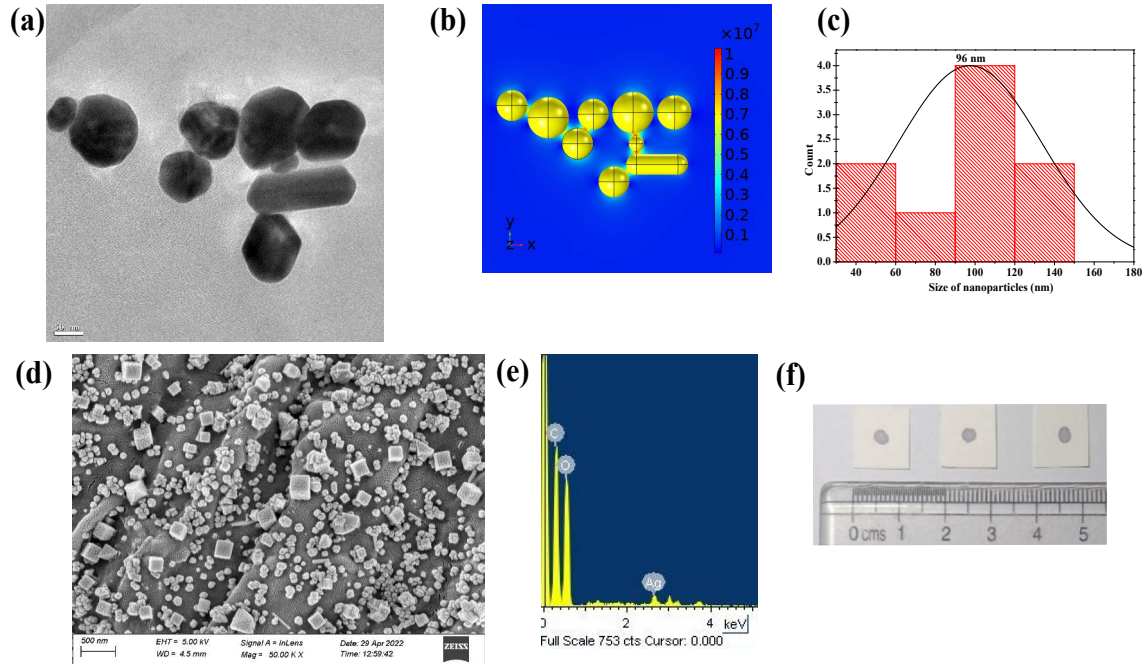

Figure 2.2: (a) TEM image of the AgNPs (b) Simulation of LSPR field of magnitude for different sized AgNPs over the 100 GSM paper substrate assuming incident electric field amplitude as 6.17×10^4 Vm^{-1} (c) Histogram of the TEM image (d) FESEM image of AgNP distribution over the 100 GSM paper substrate (Scale bar is 500 nm) (e) EDX spectra of the 100 GSM substrate showing the elements present (f) Diffusion of AgNPs on the paper substrate

citrate solution was introduced into the heated $AgNO_3$ solution. The resultant solution was kept at boiling temperature for 1 hour with continuous stirring. The transmission electron microscopy (TEM) image of the synthesized AgNPs is illustrated in figure 2.2 (a). Figure 2.2 (c) indicates that the average diameter of the synthesized nanoparticles measured $\sim$ 96 nm.

2.2.3 SERS substrate preparation

Compared to other GSM grade papers, the performance of 100 GSM SERS substrate is found to be superior in terms of average Raman signal intensities, enhancement and reproducibility characteristics. Therefore, 100 GSM paper has been selected as the base for SERS substrate fabrication in the present study. Initially, 10 µL of the synthesized AgNPs was carefully pipetted onto a paper substrate, resulting in diffusion over an area of approximately 62 mm^2. Figure 2.2(f) presents a photograph depicting the diffused region of AgNPs on the 100 GSM paper substrate. The paper's pore size and surface morphology significantly influence the diffusion process. Two primary diffusion modes were observed when pipetting AgNPs onto the paper substrate: in-plane and lateral diffusion. It has been noted that the laterally diffused AgNPs contribute more to the enhancement of Raman signals compared to in-plane diffusion [6]. In higher-grade GSM papers, lateral diffusion predominates over in-

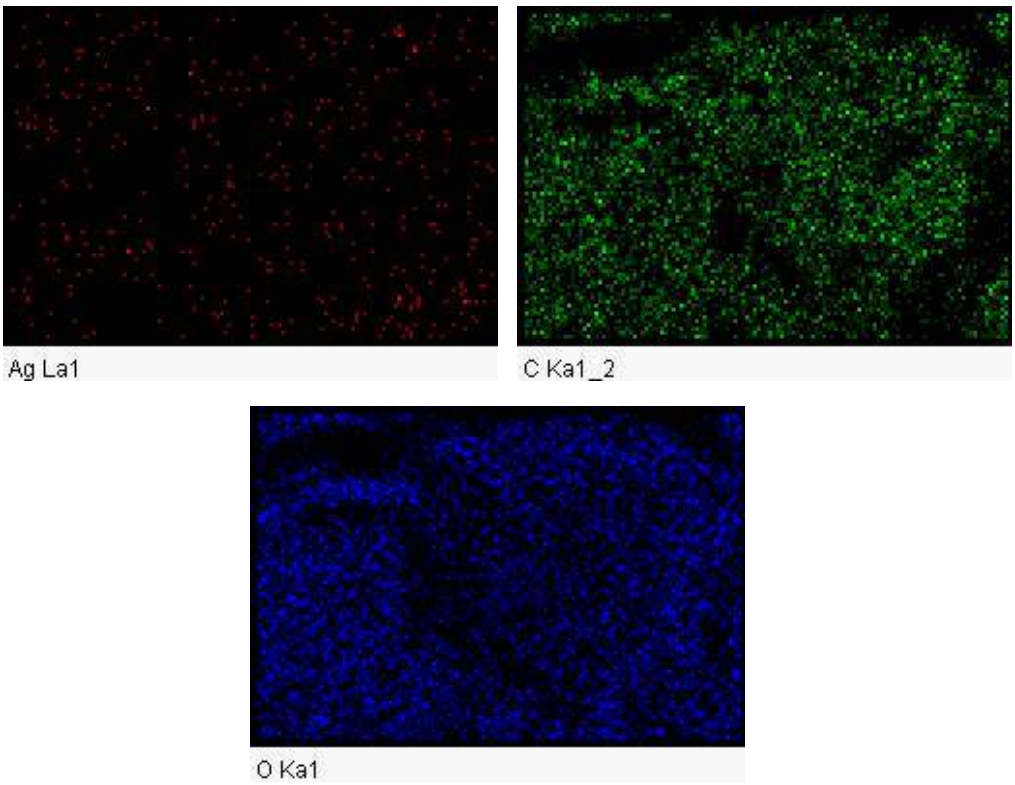

Figure 2.3: Elemental mapping of the fabricated substrate indicating the presence of silver, carbon and oxygen

plane diffusion, while for lower GSM papers, the opposite can be observed. Figure 2.2(d) displays the field emission scanning electron microscopy (FESEM) image of the 100 GSM paper substrate, revealing a uniform distribution of AgNPs across the substrate. Figure 2.2(e) presents the energy dispersive x-ray spectroscopy (EDX) data of the fabricated substrate, confirming the presence of silver in the diffusion region. Consistency in ambient conditions was maintained during the fabrication of the SERS substrate on 100 GSM paper. Furthermore, figure 2.3 illustrates the EDX-elemental mapping of the fabricated SERS substrate, indicating the uniform deposition of AgNPs over the sensing area.

2.2.4 Raman Instrument

Raman spectra have been collected using EZ-Raman-N spectrometer (Enwave opto-electronics, USA). This spectrometer is equipped with a diode laser of wavelength of 785 nm and having maximum output power of 500 mW. The spectrometer has a spectral resolution of 1.45 cm^{-1}. In the current investigation, SERS spectra were captured with the laser output power set at 5 mW. All samples were subjected to an integration time of 15 second for recording and analysis of the Raman spectra.

2.2.5 COMSOL Multiphysics simulation

To study the coupled LSPR field generated by surface-deposited AgNPs over the paper SERS substrate, a simulation study was conducted using COMSOL Multiphysics 5.2 simulation software, specifically employing its wave optics module. This simulation software utilizes the finite element method, solving Maxwell's electromagnetic equations over infinitesimal regions. To perform the simulation study, the random distribution of NPs with an average dimension of 96 nm were considered. For an incident laser at 785 nm, a maximum field amplitude of the order of $10^7\,\mathrm{Vm}^{-1}$ has been noticed at the hotspot region for the considered AgNPs. Figure 2.2(a) displays a TEM image showing the synthesized AgNPs, while figure 2.2(b) illustrates the distribution of AgNPs considered for the present simulation studies, which has been obtained from the TEM image of AgNPs as shown in figure 2.2(a). In another simulation study, the sizes of NPs were varied from 50 nm to 90 nm, maintaining a fixed separation of 5 nm between the particles, depicted in figure 2.4. For these varied particle sizes, a maximum field amplitude of 10^7 Vm^{-1} was observed. In the present simulation study the value of incident field amplitude was taken as $6.17 \times 10^4\,\mathrm{Vm}^{-1}$. The details of EF, estimated through both simulation and experimental methods, are described in table 8.16.

2.3 Results and discussion

2.3.1 Characterization of the substrate

The performance of the proposed SERS substrate was initially evaluated using two standard Raman-active samples MG and R6G respectively. Initially, 10 µL of each analyte sample, at a concentration of 1 µM, was carefully pipetted onto the sensing area of the substrate. Subsequently, the substrates were left to dry for 6 hours under ambient conditions. Upon drying, the characteristic Raman signals emitted by the samples were captured using a Raman spectrometer. The distinctive Raman spectra of MG and R6G recorded by the spectrometer are depicted in figures 2.5(a) and 2.5(b), respectively. For MG, the characteristic Raman bands ranging from 850 cm^{-1} to 1700 cm^{-1} are observed. The Raman band assignments for MG and R6G have been illustrated in tabular form in appendix section (table 8.1, table 8.2,). Different concentrations of MG and R6G have been treated with the proposed paper-based SERS substrate and the resulting Raman spectra are recorded. Figures 2.5(a) and (b) show the characteristic spectra of MG and R6G, respectively, recorded by the Raman spectrometer. Figures 2.5(c) and (d) present regression plots with regression coefficients R^2= 0.9717 and R^2 = 0.9401 for ten different concentrations of MG and R6G, respectively. These figures demonstrate a linear variation in peak intensity of

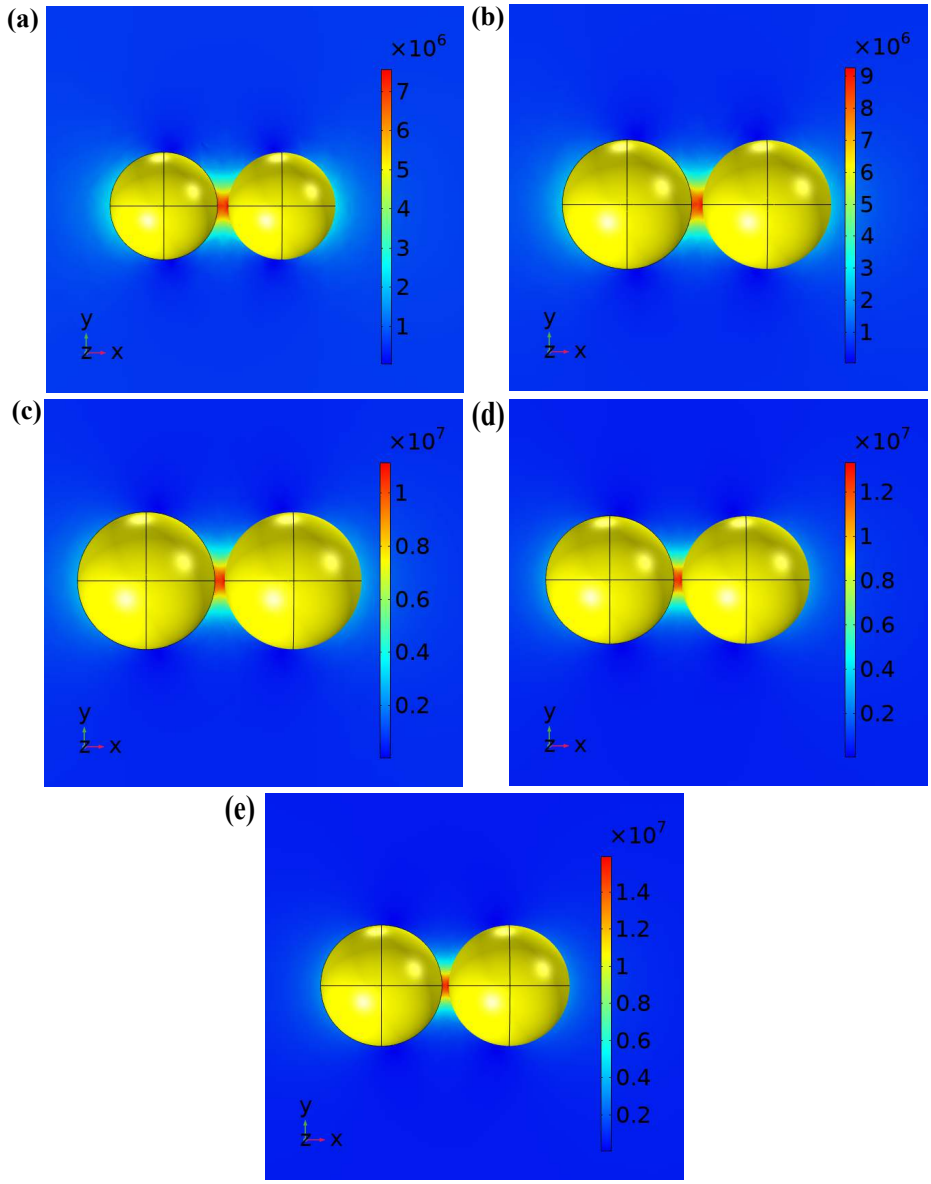

Figure 2.4: EM Simulation of two AgNPs seperated by 5 nm when the size of the NPs are (a) 50 nm (b) 60 nm (c) 70 nm (d) 80 nm (e) 90 nm; with incident electric field amplitude 6.17×10^4 Vm^{-1}

the signature Raman peaks with the samples concentration. The SERS substrate enables reliable detection of both test samples at a minimum concentration of 1 nM. These investigations underscore the capability of the fabricated SERS substrate for both qualitative and quantitative analysis of analyte samples. The Raman signals scattered from the cellulose of the paper exhibits minimal interference with the analytes signal, facilitating spectral analysis without the need for additional corrections.

2.3.2 Estimation of LoD

In the next phase of the study, LoD of the proposed sensing platform has been estimated. Ten different samples of MG ranging from 10 nM (0.00927 mgL^{-1}) to

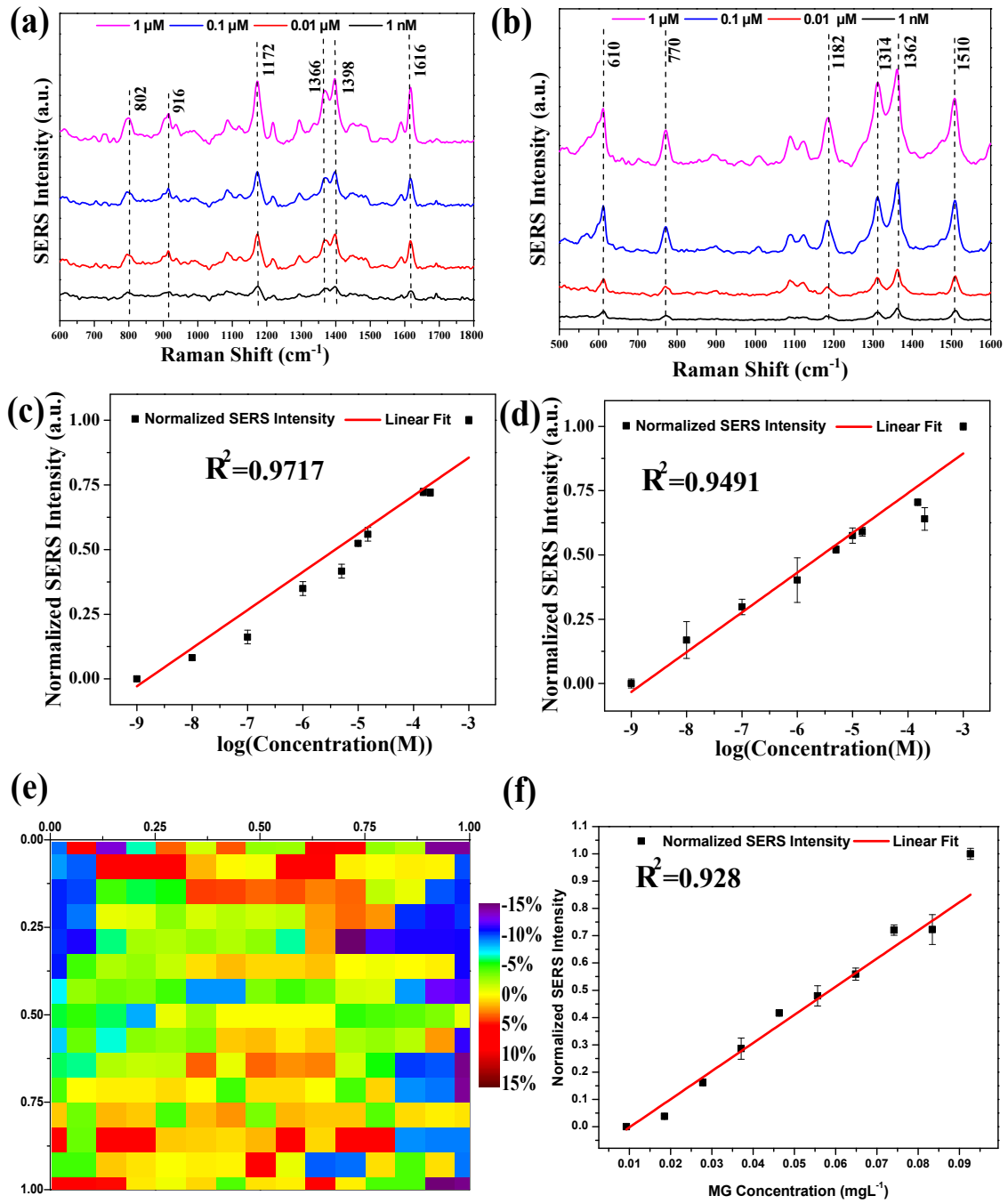

Figure 2.5: (a) Comparison of SERS spectra of MG at four different concentrations (b) Comparison of SERS spectra of R6G at four different concentrations (c) Variation of SERS intensity with different concentrations for MG at a signature Raman peak at 1398 cm^{-1} (d) Variation of SERS intensity with different concentrations for R6G at a signature Raman peak at 1362 cm^{-1} (e) SERS intensity variation in random locations of the substrate over an area of 1 mm × 1 mm corresponding to the Raman peak at 1398 cm^{-1} (f) Normalized SERS signal intensity variation of the MG solution corresponding to the Raman peak at 1398 cm^{-1} for the concentrations 0.00927 mgL^{-1}−0.0927 mgL^{-1}; (Error bars are plotted using the standard deviation, calculated from five repetitions for each sample)

100 nM (0.0927 mgL^{-1}) have been considered , in incremental steps of 10 nM to evaluate this parameter. Each of these samples has been treated individually with the fabricated substrates, and the resulting backscattered Raman signal intensities were recorded. Figure 2.5(f) illustrates the variations in normalized SERS signal intensity of the signature Raman peak at 1398 cm^{-1}. From the characteristic curve depicted in the figure, the LoD was determined using the following equation [30]:

$$LoD = \frac{3.3\sigma}{S} \tag{2.1}$$

where, σ represents the standard deviation of the y-intercepts, and S denotes the slope of the linear fitted line. The estimated LoD for the designed substrate was calculated to be 0.03386 mgL^{-1} ($\sim$ 92.7 nM).

2.3.3 Uniformity and reproducibility study

The uniformity of the fabricated SERS substrate was assessed using MG as the analyte. In this investigation, 1 µM of MG was carefully pipetted onto the sensing region of the substrate of the substrate and the scattered Raman signals were then recorded across an area of 1 mm $\times$ 1 mm. The results are depicted in figure 2.5(e). To analyze the uniformity characteristics of the SERS substrate, the characteristic Raman peak of MG at 1398 cm^{-1} has been selected. For the considered sensing region, a maximum SERS signal variations of 15% has been observed, suggesting a good degree of uniformity characteristics of the designed SERS platform. Furthermore, the reproducibility of the substrate was assessed using both MG and R6G. Figure 2.6(a) and (b) illustrates the reproducibility analysis for MG and R6G respectively. Figure 2.6(c) depicts the study on spectral uniformity of the designed SERS substrate, where 1 µM of MG sample was applied onto the sensing region, and spectra were recorded at 21 random points on the same substrate. The Raman probe records the scattered Raman signal from an area of approximately 14.41 μm^2 which implies that the backscattered signals are being recorded from an area that contain a large number of hotspots regions. Thus, despite the heterogeneous nature of the synthesized nanoparticles the spectrometer records an average signal intensity from the sensing region of the SERS substrate and not from the individual hotspot region. The averaged signal intensity leads to good degree of reproducibility.

2.3.4 Estimation of EF

In the next step of the present work, the EF of the proposed paper-based SERS substrate was estimated using the following equations:

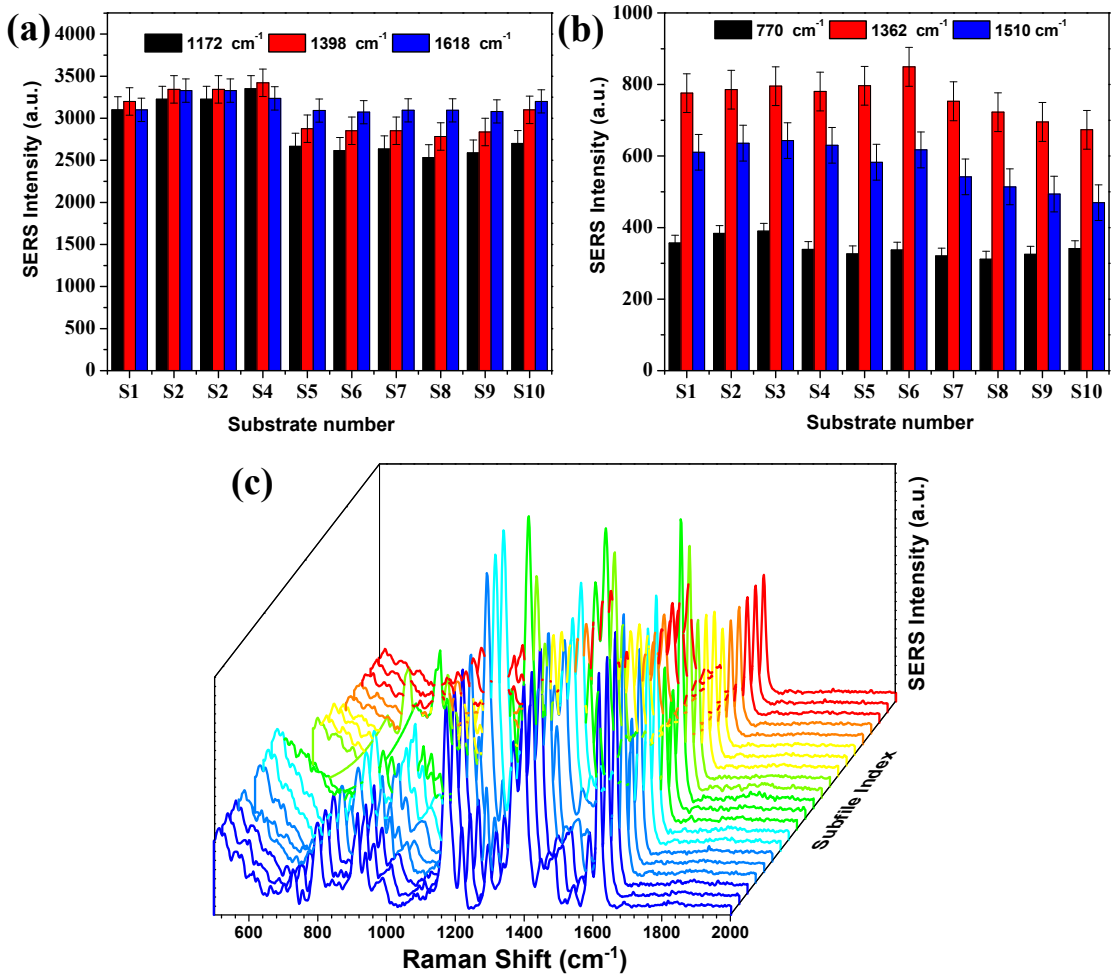

Figure 2.6: (a) Reproducibility characteristics of MG for ten different substrates (b) Reproducibility characteristics of R6G for ten different substrates (c) Uniformity of the substrate, evaluated by taking 21 random locations of the substrate; (Error bars are plotted using the standard deviation, calculated from five repetitions for each sample)

$$EF = \frac{I_{SERS} \times N_{REF}}{I_{REF} \times N_{SERS}} \tag{2.2}$$

where, I_{SERS} and I_{REF} represent the backscattered Raman signal intensities of the sample from the SERS substrate and reference substrate, respectively. Similarly, N_{SERS} and N_{REF} denote the number of molecules present within the laser excitation area of the SERS substrate and reference substrate, respectively. The value of N_{REF} and N_{SERS} was determined using the following equation

$$N_{REF} = VCN_A \tag{2.3}$$

$$N_{SERS} = \frac{C_{SERS}V_{SERS}AN_A}{S} \tag{2.4}$$

where V and V_{SERS} represent the volumes of the analyte solution used for obtaining the SERS and reference Raman spectra, respectively. C and C_{SERS} denote the molar

concentrations of the analyte employed in the SERS and reference Raman spectra measurements. A refers to the area of the laser spot, S is the total surface area covered by analyte molecules on the substrate, and N_A is Avogadros number. A uniform distribution of analyte molecules across the SERS substrate has been considered. The value of N_{REF} was calculated to be 3.4021×10^7 for a laser spot size with a diameter of 4.353 µm. The spot size of the laser was calculated using the following equation

$$spot\ size = \frac{1.22\lambda}{NA} \tag{2.5}$$

where NA denotes the numerical aperture of the objective lens. To determine the reference Raman signal intensities, 10 mM of MG was dispensed onto a plain 100 GSM paper substrate. Utilizing equation 2.2, the experimental EF was estimated to be approximately $\sim 10^7$. The value of N_{SERS} was determined considering monolayer distribution of MG sample over the SERS substrate. The value of N_{SERS} can be obtained by using the following equation [31, 32].

2.3.5 SERS detection of pharmaceutical drugs

Upon noticing reliable performance with standard Raman-active samples, the applicability of the SERS substrate has been realized through detecting pharmaceutical drugs, specifically paracetamol and aspirin, in water. Both paracetamol and aspirin exhibit low solubility in water. To prepare a stock solution of 1 mM, 15.1 mg of paracetamol was dissolved in 100 mL of deionized water (DI water). Additionally, two different paracetamol samples with concentrations of 0.5 mM and 0.1 mM were prepared by diluting the stock solution with a proportional amount of DI water. Subsequently, 10 µL each of the prepared sample was pipetted over the SERS substrate and allowed to dry in room temperature conditions. Figure 2.7(a) displays the Raman spectra of the SERS substrate in the absence of drugs, while figure 2.7(b) illustrates the characteristic Raman spectra of the paracetamol sample detected from the paper substrate. The figure also includes the Raman spectra of other two samples considered for the present investigation. The band assignment for paracetamol has been illustrated in the appendix section (table 8.4) [22]. Figure 2.7(d) shows the regression plot with regression coefficient values $R^2 = 0.959$ for ten different concentrations of paracetamol. Notably, the intensities of the signature Raman peaks exhibit gradual variations with decreasing concentrations of paracetamol in the solution. In the subsequent step, a stock solution of 1 mM was prepared by dissolving 18.0 mg of aspirin in DI water. Four different concentrations of aspirin (1 mM, 0.5 mM, 0.3 mM, and 0.1 mM) were prepared by diluting the stock samples accordingly. 10 µL each of the different aspirin concentration sample was dispensed separately onto the SERS substrates and the Raman signal analysis was conducted. Figure 2.7(c) shows the

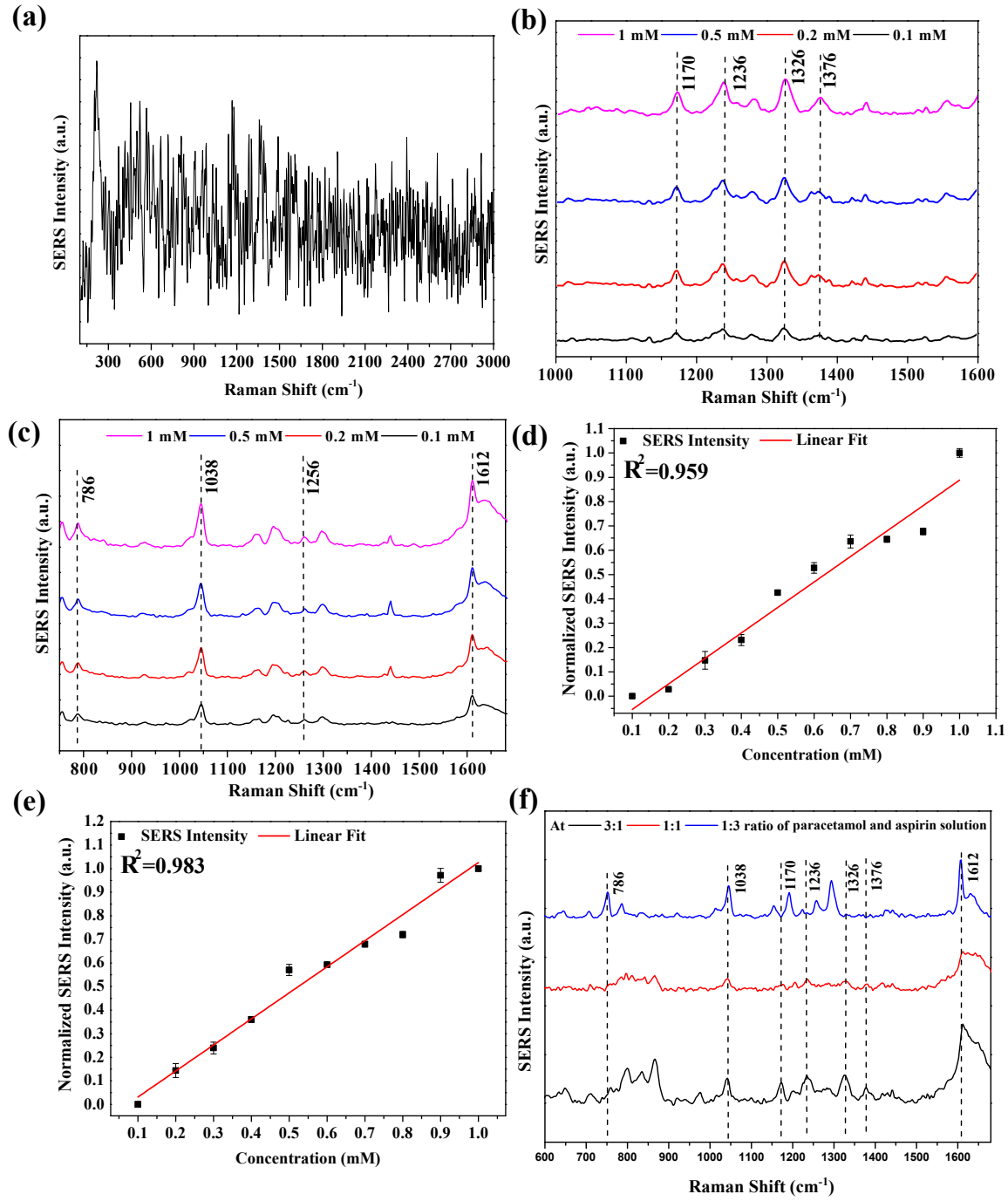

Figure 2.7: (a) Recorded Raman spectra in the absence of pharmaceutical drugs, relative Raman signal intensities of different concentrations of (b) paracetamol and (c) aspirin in water, variation of SERS signal intensity at different concentrations at the signature Raman peak of (d) paracetamol at 1326 cm^{-1} and (e) aspirin at 1038 cm^{-1} and (f) SERS spectra of the mixed analytes of paracetamol and aspirin in three different concentration ratios; (Error bars are plotted using the standard deviation, calculated from five repetitions for each sample)

characteristic Raman spectra obtained from the aspirin-treated SERS substrate. Distinctive Raman peaks of aspirin were observed at 786 cm^{-1}, 1038 cm^{-1}, 1256 cm^{-1}, and 1612 cm^{-1}. The characteristics Raman bands for aspirin have been described in table 8.5 of appendix. [27–29]. Figure 2.7(e) depicts the regression plot with a regression coefficient value of $R^2 = 0.983$ for ten different aspirin concentrations. A gradual variation in the scattered signal intensity has been observed with the concentrations of aspirin in the water medium. These results show that with the proposed SERS sensing platform quantitative analysis of pharmaceutical drugs in water could be performed. The LoD for both considered pharmaceutical drug samples was estimated and the values were found to be 0.1 mM for each sample. The estimated LoDs are found to be lower than the values reported elsewhere [22–27]. Table 2.1 summarizes the comparison of LoD values obtained from the present approach with those reported in previous studies for the two considered pharmaceutical drugs.

Table 2.1: Comparison of the LoDs of previously reported works and the present work on sensing of paracetamol and aspirin.

Analytes	Substrate used	Matrices	LoD	Reference
Paracetamol	AuNP-chitosen deposited on glass substrate	Aqueous medium	1 mM	[22]
	Commercial AuNP at Al foil	Aqueous medium	24 mM	[23]
Aspirin	Colloidal solution AgNP and AuNP	Blood serum	3 mM	[26]
	AgNP coated filter paper	Ethanol	0.1 mM	[29]

In the next step of the present study, a mixed sample comprising paracetamol and aspirin have been dissolved in DI water were analysed at three distinct concentration ratios (paracetamol: aspirin, 3:1, 1:1, and 1:3, respectively). The scattered Raman signals from the sensing region of the substrate for these mixed samples has been presented in figure 2.7(f). The characteristic Raman peaks of paracetamol and aspirin at 1326 cm^{-1} and 786 cm^{-1} demonstrate variations corresponding to the ratio of the analytes in the mixture. These variations suggest that the peaks exhibit intensity changes in response to the variations in the concentration of the analytes. Specifically, for higher concentrations of paracetamol in the mixture, the characteristic Raman peaks at 1236 cm^{-1}, 1326 cm^{-1}, and 1376 cm^{-1} gradually vary with its concentration. Conversely, the signature Raman peaks of aspirin at 786 cm^{-1}, 1038 cm^{-1}, and 1612 cm^{-1} are found to be varying proportionally with its concentration in the mixture. The presence of molecules of the second pharmaceutical drug in the medium perturbs other Raman peaks of both samples. These investigations suggest that with the designed SERS platform detection and quantification of a specific pharmaceutical drug from a mixed sample can be performed reliably, thus offering

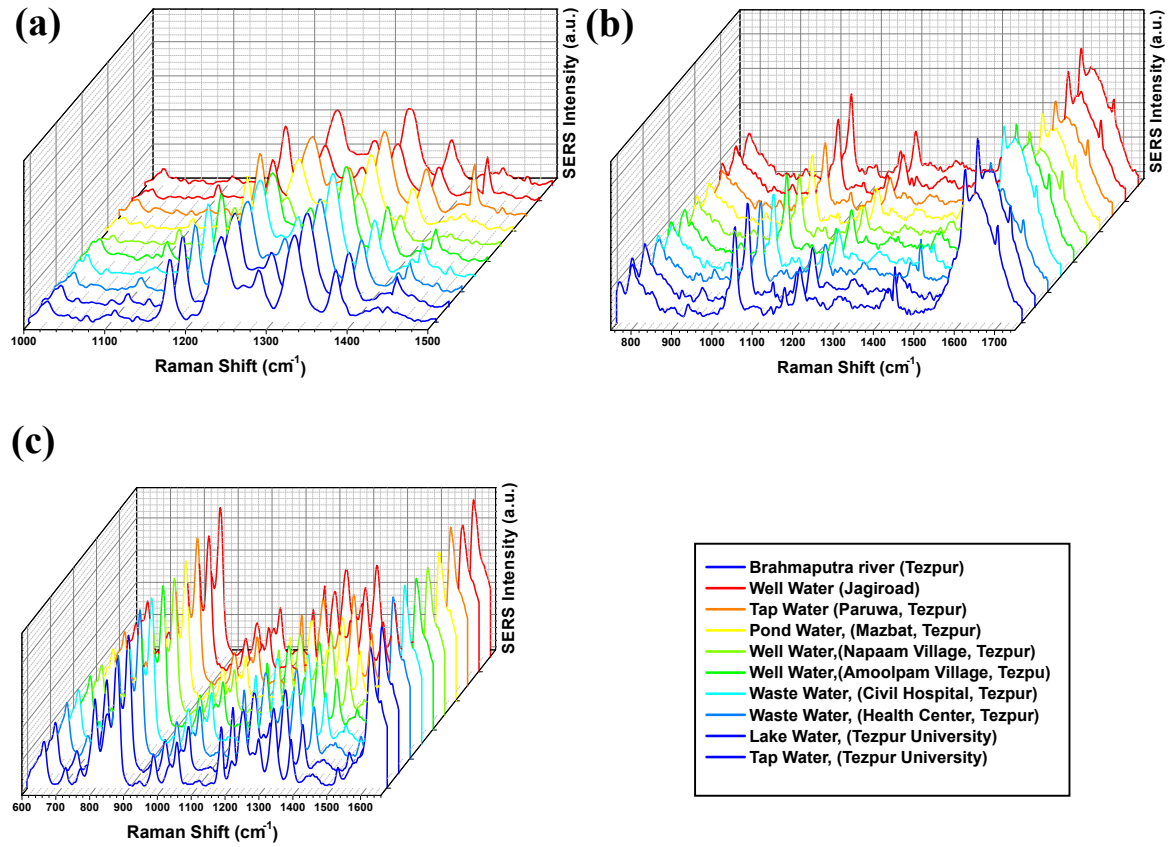

Figure 2.8: SERS spectra of the field-collected sample (a) with paracetamol (b) with aspirin (c) in a 1:1 concentration ratio of the mixed solution of paracetamol to aspirin in the ten field-collected water samples collected from ten different regions

potential applications in the analysis of pharmaceutical drugs.

2.3.6 Real Sample analysis

In the final part of the present sensing study, the practical utility of the proposed sensing technique has been demonstrated through detection of pharmaceutical drugs in real water samples collected from various sources. Samples from ten distinct water resources were obtained for this purpose. No detectable spectra of the target analytes was observed in field-collected samples. The samples were then spiked with a fixed concentration of analytes. Prior to dissolving the pharmaceutical drugs, all field-collected samples were filtered using grade-1 Whatman filter paper. 0.5 mM each of pharmaceutical drugs has been added to different field-collected water samples. A mixed solution containing paracetamol and aspirin in 1:1 ratio has been prepared in the field-collected water samples. Figures 2.8(a)-(c) illustrate the characteristic Raman spectra of paracetamol, aspirin, and the mixed sample, respectively, as recorded by the Raman spectrometer. The bottom right panel in figure 2.8 presents color-coded labels representing the various field-collected water samples acquired for this study. The figure demonstrates a reliable detection of characteristic Raman peaks

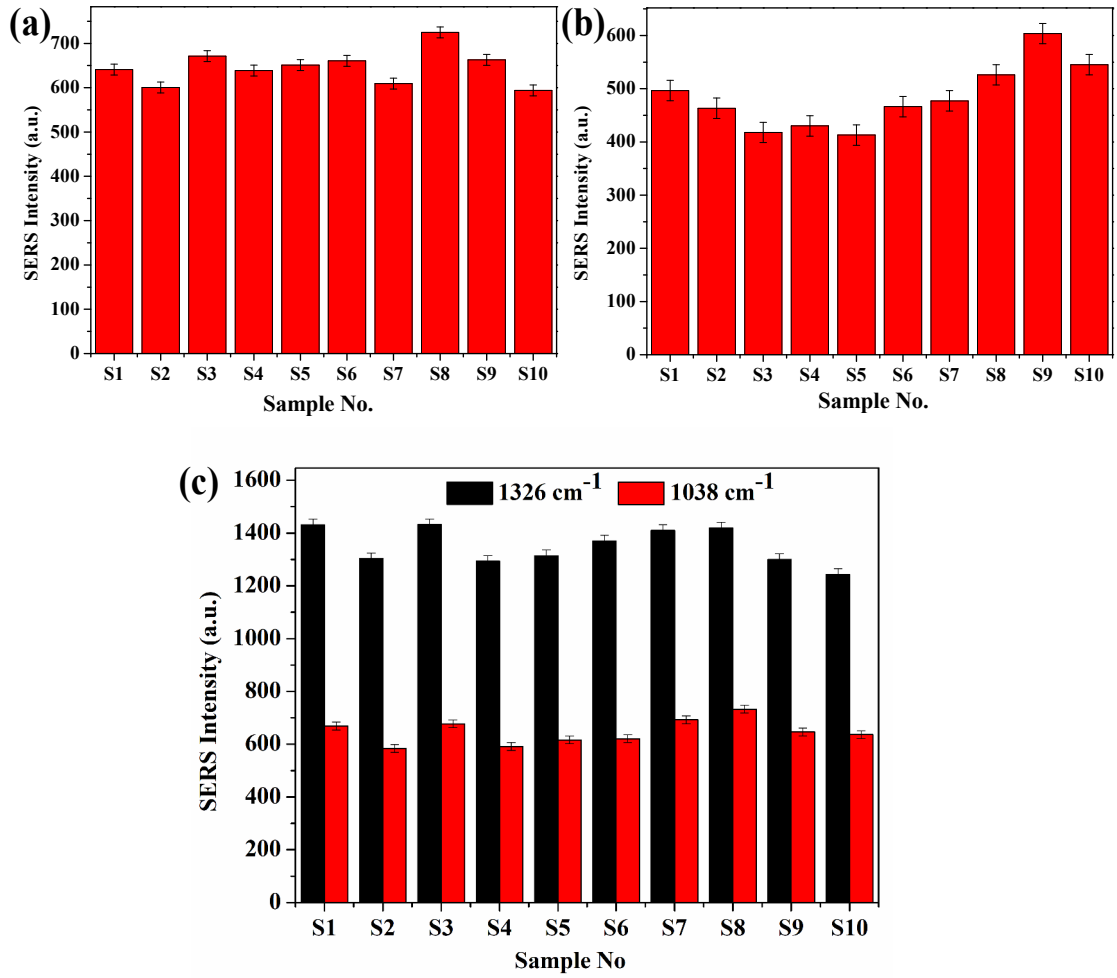

Figure 2.9: Peak intensity variation corresponding to peak at (a) 1326 cm^{-1} for paracetamol and (b) 1038 cm^{-1} for aspirin (c) Peak intensity variation corresponding to peak at 1326 cm^{-1} for paracetamol and 1038 cm^{-1} for aspirin for 1:1 concentration ratio of the mixed solution of paracetamol to the aspirin;(Error bars are plotted using the standard deviation, calculated from five repetitions for each sample)

of the analyzed pharmaceutical drugs using the proposed technique, regardless of whether they are present individually or in a mixed form. From figure 2.8(c), it is evident that the characteristic Raman peaks of paracetamol at 1170 cm^{-1}, 1236 cm^{-1}, 1326 cm^{-1}, and 1376 cm^{-1} are prominently visible. Similarly, for aspirin, the signature Raman peaks at 786 cm^{-1}, 1038 cm^{-1}, 1256 cm^{-1}, and 1612 cm^{-1} consistently appear across all field-collected water samples, when they are present in a mixed form. This study reveals the capability of current sensing technique to detect pharmaceutical drugs in water samples, even when the drug components are present mixed form. The variations in Raman signal intensities of the targeted pharmaceutical drugs in field-collected water samples were further examined and are depicted in figure 2.9. To assess the variations of the recorded Raman signals, the characteristic Raman peaks of paracetamol and aspirin at 1326 cm^{-1} and 1038 cm^{-1}, respectively, were examined. Figures 2.9(a) and 2.9(b) display the fluctuations in Raman signal

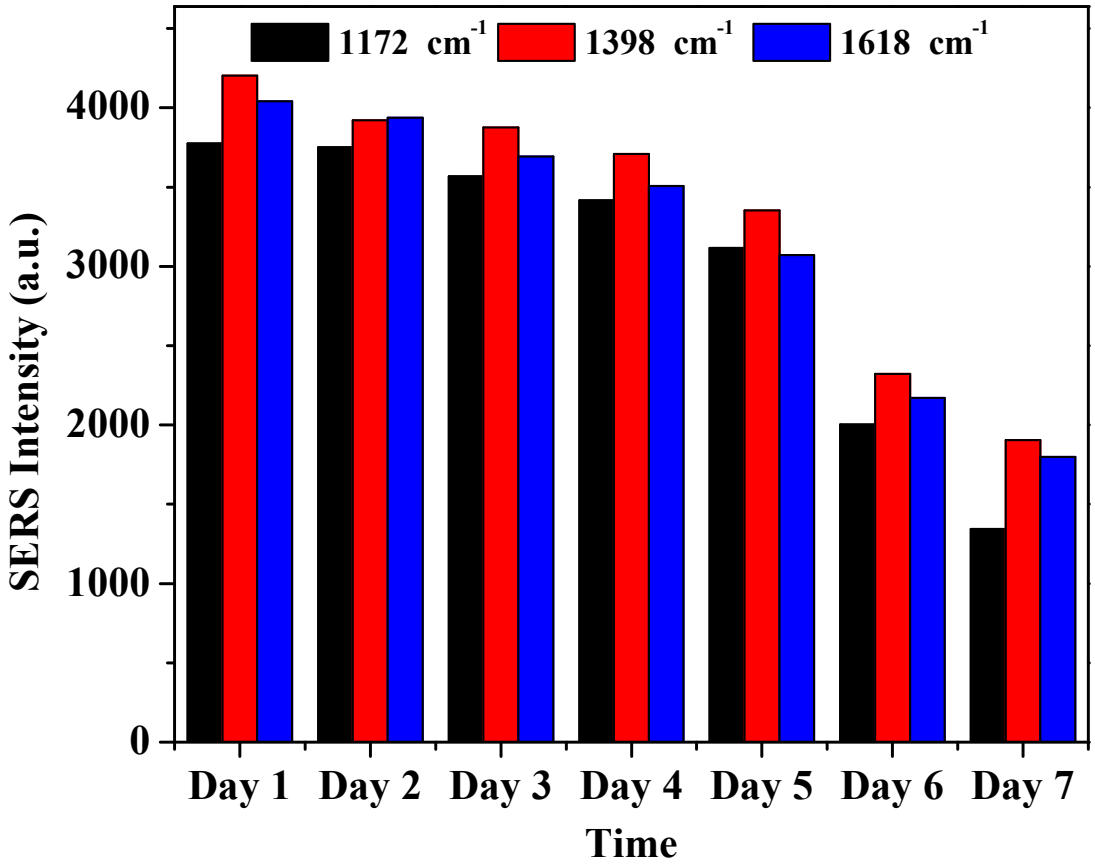

Figure 2.10: Time evaluation study of the fabricated substrate

intensity at these two peaks as recorded by the Raman spectrometer. The relative standard deviation (RSD) values for the peaks corresponding to paracetamol at 1326 cm^{-1} and aspirin at 1038 cm^{-1} are found to be $\sim$ 9% and 12%, respectively, from their respective mean values. Similarly, for the mixed sample, the signature peaks at 1326 cm^{-1} and 1038 cm^{-1} demonstrate RSD values of 11% and 13%, respectively, as shown in figure 2.9(c). The low RSD values indicate uniformity in Raman signal intensity across ten different field-collected samples. This study confirms the practical applicability of the method for sensing pharmaceutical drugs in aqueous media.

2.3.7 Time evaluation study

A temporal evaluation of the proposed SERS platform has been performed to examine the fluctuations with time. Figure 2.10 presents the results of this time evaluation study performed on the designed SERS platform for 7 consecutive days. It has been observed that the intensity of the scattered Raman signal from the analyte sample remained relatively stable in the initial four days, however a gradual decrement in the SERS intensity was noted after the fifth day. This observation suggests that the proposed approach maintains reliability for sensing investigations within approxi-

mately 100 hours from the time of substrate fabrication. Conversely, SERS substrates treated with AuNPs are anticipated to exhibit a comparatively prolonged duration of stable performance. The method yields a favourable signal-to-noise ratio, rendering it suitable for detecting and analysing various pharmaceutical drugs and toxic chemicals in water. The fabrication cost of the proposed SERS substrate is remarkably low, approximately INR 5.00 (<$0.067), thus can be used for disposable sensing studies. With potential for large-scale production, the cost could be further reduced. Additionally, the fabrication process proposed here is straightforward, allowing to fabricate SERS substrates within a standard laboratory environment.

2.4 Summary

This present chapter demonstrates a cost-effective yet an acceptably sensitive SERS substrate fabrication method. The usability of the proposed sensing platform has been showed to detect two pharmaceutical compounds, namely paracetamol and aspirin in water. The well-established Lee-Meisel technique has been employed to synthesize AgNPs in the laboratory, resulting in an average SERS EF of $\sim 10^7$. Subsequently, we devised a paper-based SERS substrate by depositing AgNPs onto 100 GSM grade paper through drop-casting. Notably, the substrate exhibits a good reproducibility characteristics. The fluctuations in the scattered Raman signal intensity was found to be maximum $\sim 15\%$, indicating a good spectral uniformity across the substrate. The present study successfully demonstrates the capability of detecting and quantifying both paracetamol and aspirin in diverse aqueous environments, including DI and field-collected water samples. This technique possesses versatility beyond pharmaceutical compounds, as the same technique can be also used to detect other toxic chemicals present in water.

References

[1] Chamuah, N., Saikia, A., Joseph, A. M., and Nath, P. Blu-ray DVD as SERS substrate for reliable detection of albumin, creatinine and urea in urine. *Sensors and Actuators B: Chemical*, 285:108–115, 2019. ISSN 0925-4005.

[2] Lee, M., Oh, K., Choi, H.-K., Lee, S. G., Youn, H. J., Lee, H. L., and Jeong, D. H. Subnanomolar Sensitivity of Filter Paper-Based SERS Sensor for Pesticide Detection by Hydrophobicity Change of Paper Surface. *ACS Sensors*, 3(1):151–159, Jan. 2018. doi: 10.1021/acssensors.7b00782. URL https://doi.org/10.1021/acssensors.7b00782. Publisher: American Chemical Society.

[3] Huang, J.-A., Zhang, Y.-L., Zhao, Y., Zhang, X.-L., Sun, M.-L., and Zhang, W. Superhydrophobic SERS chip based on a Ag coated natural taro-leaf. *Nanoscale*, 8(22):11487–11493, 2016. Number: 22.

[4] Yao, L., Dai, P., Ouyang, L., and Zhu, L. A sensitive and reproducible SERS sensor based on natural lotus leaf for paraquat detection. *Microchemical Journal*, 160:105728, 2021. Publisher: Elsevier.

[5] Pan, X., Bai, L., Pan, C., Liu, Z., and Ramakrishna, S. Design, Fabrication and Applications of Electrospun Nanofiber-Based Surface-Enhanced Raman Spectroscopy Substrate. *Critical Reviews in Analytical Chemistry*, pages 1–20, 2021. Publisher: Taylor & Francis.

[6] Chamuah, N., Hazarika, A., Hatiboruah, D., and Nath, P. SERS on paper: an extremely low cost technique to measure Raman signal. *Journal of Physics D: Applied Physics*, 50(48):485601, 2017. Number: 48 Publisher: IOP Publishing.

[7] Monteiro, M. K. S., Santos, E. C. M. M., Silva, D. R., Martínez-Huitle, C. A., and dos Santos, E. V. Simultaneous determination of paracetamol and caffeine in pharmaceutical formulations and synthetic urine using cork-modified graphite electrodes. *Journal of Solid State Electrochemistry*, 24(8):1789–1800, 2020. Number: 8 Publisher: Springer.

[8] Shaban, S. M., Moon, B.-S., and Kim, D.-H. Selective and sensitive colorimetric detection of p-aminophenol in human urine and paracetamol drugs based on seed-mediated growth of silver nanoparticles. *Environmental Technology & Innovation*, 22:101517, 2021. Publisher: Elsevier.

[9] Paroji, J., Karljikovi-Raji, K., Duri, Z., Jovanovi, M., and Ibri, S. Development of the second-order derivative UV spectrophotometric method for direct determination of paracetamol in urine intended for biopharmaceutical characterisation of drug products. *Biopharmaceutics & drug disposition*, 24(7):309–314, 2003. Publisher: Wiley Online Library.

[10] Zwiener, C., Glauner, T., and Frimmel, F. H. Biodegradation of pharmaceutical residues investigated by SPE-GC/ITD-MS and on-line derivatization. *Journal of High Resolution Chromatography*, 23(7-8):474–478, 2000. Number: 7-8 Publisher: Wiley Online Library.

[11] Buser, H.-R., Poiger, T., and Müller, M. D. Occurrence and environmental behavior of the chiral pharmaceutical drug ibuprofen in surface waters and in wastewater. *Environmental science & technology*, 33(15):2529–2535, 1999. Number: 15 Publisher: ACS Publications.

[12] Ebele, A. J., Abdallah, M. A.-E., and Harrad, S. Pharmaceuticals and personal care products (PPCPs) in the freshwater aquatic environment. *Emerging Contaminants*, 3(1):1–16, 2017. Number: 1 Publisher: Elsevier.

[13] Bedner, M. and MacCrehan, W. A. Transformation of acetaminophen by chlorination produces the toxicants 1, 4-benzoquinone and N-acetyl-p-benzoquinone imine. *Environmental science & technology*, 40(2):516–522, 2006. Number: 2 Publisher: ACS Publications.

[14] Cao, F., Zhang, M., Yuan, S., Feng, J., Wang, Q., Wang, W., and Hu, Z. Transformation of acetaminophen during water chlorination treatment: kinetics and transformation products identification. *Environmental Science and Pollution Research*, 23(12):12303–12311, 2016. Number: 12 Publisher: Springer.

[15] Amann, R. and Peskar, B. A. Anti-inflammatory effects of aspirin and sodium salicylate. *European journal of pharmacology*, 447(1):1–9, 2002. Number: 1 Publisher: Elsevier.

[16] Vainio, H. and Morgan, G. Aspirin for the second hundred years: new uses for an old drug. *Pharmacology & toxicology*, 81(4):151–152, 1997. Number: 4 Publisher: Wiley Online Library.

[17] Vane, J. R. and Botting, R. M. The mechanism of action of aspirin. *Thrombosis research*, 110(5-6):255–258, 2003. Number: 5-6 Publisher: Elsevier.

[18] Moldovan, Z. Occurrences of pharmaceutical and personal care products as micropollutants in rivers from Romania. *Chemosphere*, 64(11):1808–1817, 2006. Number: 11 Publisher: Elsevier.

[19] Glassmeyer, S. T. and Shoemaker, J. A. Effects of chlorination on the persistence of pharmaceuticals in the environment. *Bulletin of environmental contamination and toxicology*, 74(1):24–31, 2005. Number: 1 Publisher: Springer.

[20] Bufan, B., Mojsilovi, S., Vuievi, D., Vuevi, D., Vasiliji, S., Balint, B., and oli, M. Comparative effects of aspirin and NO-releasing aspirins on differentiation, maturation and function of human monocyte-derived dendritic cells in vitro. *International immunopharmacology*, 9(7-8):910–917, 2009. Number: 7-8 Publisher: Elsevier.

[21] Campbell, E. J. M. and Maclaurin, R. E. Acute renal failure in salicylate poisoning. *British medical journal*, 1(5069):503, 1958. Number: 5069 Publisher: BMJ Publishing Group.

[22] de Barros Santos, E., Lima, E. C. N. L., de Oliveira, C. S., Sigoli, F. A., and Mazali, I. O. Fast detection of paracetamol on a gold nanoparticlechitosan substrate by SERS. *Analytical Methods*, 6(11):3564–3568, 2014. Publisher: Royal Society of Chemistry.

[23] Mukanova, Z., Gudun, K., Elemessova, Z., Khamkhash, L., Ralchenko, E., and Bukasov, R. Detection of paracetamol in water and urea in artificial urine with gold nanoparticle@ Al foil cost-efficient SERS substrate. *Analytical Sciences*, 34(2):183–187, 2018. Number: 2 Publisher: The Japan Society for Analytical Chemistry.

[24] Decorbie, N., Tijunelyte, I., Gam-Derouich, S., Solard, J., Lamouri, A., Decorse, P., Felidj, N., Gauchotte-Lindsay, C., Rinnert, E., Mangeney, C., and others. Sensing Polymer/Paracetamol Interaction with an Independent Component Analysis-Based SERS-MIP Nanosensor. *Plasmonics*, 15(5):1533–1539, 2020. Number: 5 Publisher: Springer.

[25] Sanger, K., Durucan, O., Wu, K., Thilsted, A. H., Heiskanen, A., Rindzevicius, T., Schmidt, M. S., Zór, K., and Boisen, A. Large-scale, lithography-free production of transparent nanostructured surface for dual-functional electrochemical and SERS sensing. *ACS sensors*, 2(12):1869–1875, 2017. Number: 12 Publisher: ACS Publications.

[26] El-Zahry, M. R., Refaat, I. H., Mohamed, H. A., and Lendl, B. Sequential SERS determination of aspirin and vitamin C using in situ laser-induced photochemical silver substrate synthesis in a moving flow cell. *Analytical and bioanalytical chemistry*, 408(17):4733–4741, 2016. Number: 17 Publisher: Springer.

[27] Adomaviit, S., Velika, M., and ablinskas, V. Detection of aspirin traces in blood by means of surface-enhanced Raman scattering spectroscopy. *Journal of Raman Spectroscopy*, 51(6):919–931, 2020. Publisher: Wiley Online Library.

[28] Yarantseva, N. D., Belyatsky, V. N., Shleiko, E. V., Osotskaya, E. S., Burko, A. A., Dolgiy, A. L., Girel, K. V., and Bandarenka, H. V. Detection of ibuprofen and aspirin on silver nets by surface enhanced Raman scattering (SERS) spectroscopy. In *Journal of Physics: Conference Series*, volume 1866, page 012007. IOP Publishing, 2021.

[29] Sallum, L. F., Soares, F. L. F., Ardila, J. A., and Carneiro, R. L. Determination of acetylsalicylic acid in commercial tablets by SERS using silver nanoparticle-coated filter paper. *Spectrochimica Acta Part A: Molecular and Biomolecular Spectroscopy*, 133:107–111, 2014. Publisher: Elsevier.

[30] Chamuah, N., Bhuyan, N., Das, P. P., Ojah, N., Choudhary, A. J., Medhi, T., and Nath, P. Gold-coated electrospun PVA nanofibers as SERS substrate for detection of pesticides. *Sensors and Actuators B: Chemical*, 273:710–717, 2018. Publisher: Elsevier.

[31] Le Ru, E. C., Blackie, E., Meyer, M., and Etchegoin, P. G. Surface enhanced raman scattering enhancement factors: a comprehensive study. *The Journal of Physical Chemistry C*, 111(37):13794–13803, 2007.

[32] Xiao, G.-N., Huang, W.-B., and Li, Z.-H. Rapid and sensitive detection of malachite green and melamine with silver film over nanospheres by surface-enhanced raman scattering. *Plasmonics*, 12:1169–1175, 2017.